JOURNAL OF MATERIALS SCIENCE 23 (1988) 577–582

High-temperature deformation and fracture behaviour of Cu–SiO_2 bicrystals

SUSUMU ONAKA*, SATOSHI SOETA, MASAHARU KATO, RYOHEI TANAKA‡
Department of Materials Science and Engineering, Tokyo Institute of Technology, 4259 Nagatsuta, Midori-ku, Yokohama 227, Japan

Bicrystals of Cu–SiO_2 dispersion-hardened alloys and of pure copper were tensile tested at various temperatures between 450 and 1050 K at a strain rate of $1.5 \times 10^{-4}\,sec^{-1}$. In the case of pure copper bicrystals, elongation to fracture did not depend significantly on temperature and the fracture mode was invariably transgranular up to 850 K. On the other hand, the ductility of Cu–SiO_2 bicrystals decreased with increase in temperature and the transition in the fracture mode from transgranular to intergranular occurred at around 450 K. SiO_2 particles on grain boundaries play an important role on intergranular fracture by suppressing grain-boundary sliding and also on the retardation of recrystallization during deformation. Two types of Cu–SiO_2 bicrystals having different crystal orientation relationships show quite different deformation and fracture behaviour. This can be explained in terms of the contribution of lattice dislocations to the grain-boundary sliding.

1. Introduction

When grain-boundary sliding occurs actively at high temperatures, many phenomena, characteristic of high-temperature deformation, occur around boundaries. Because of the concentration of deformations at grain boundaries, recrystallization during deformation is often confined to boundary regions [1]. Moreover, because dispersoids on grain boundaries block the sliding, stress concentration occurs at the grain boundary, which induces the formation of voids to cause intergranular fracture [2, 3].

In order to reveal the effects of grain-boundary dispersoids and inclusions on the grain-boundary sliding and on the phenomena related to high-temperature deformation, some investigations have been made using dispersion-hardened alloys. Pavinich and Raj [4] studied the deformation and fracture behaviour of Cu–SiO_2 dispersion-hardened alloys at high temperatures, and Onaka *et al.* [5] studied that of Cu–GeO_2 alloys in an intermediate temperature range. Although some aspects of the role of the grain-boundary particles on high-temperature deformation and fracture have been clarified by their studies, the use of polycrystals in their experiments prohibited us from examining the interrelationship between grain-boundary sliding, crystal deformation and intergranular fracture for a particular grain boundary.

In the present study, the deformation and fracture behaviour of copper bicrystals with dispersed silica (SiO_2) particles on grain boundaries will be examined. By using bicrystals, the deformation and fracture behaviour of a particular grain boundary can be extracted from experimental results.

2. Experimental details

2.1. Specimen preparation

From as-rolled Cu–0.1 mass % Si alloy sheets, bicrystals of Cu–Si with a macroscopically planar grain boundary were grown by the Bridgman method. In order to obtain SiO_2 dispersed particles in the grains and on the grain boundary, these bicrystals were internally oxidized with a Cu–Cu_2O–Al_2O_3 (mass ratio 1 : 1 : 2) mixed powder at 1123 K for 2.16×10^5 sec. Thereby, two Cu–SiO_2 bicrystals (samples I and II), having different orientation relationships between two grains, were obtained. By analysing back-reflection X-ray Laue photographs, it was found that neither of these two orientation relationships could be explained by the coincident site lattice model up to $\Sigma = 25$. Therefore, the grain boundaries of these two Cu–SiO_2 bicrystals were identified as the so-called random ones [6].

The average radii, r, and area fractions, A, of SiO_2 particles on grain boundaries in samples I and II were measured from scanning electron micrographs of fracture surfaces. As tabulated in Table I, samples I and II have approximately the same size and distribution of grain-boundary particles.

For comparison, a bicrystal of pure copper having a planar and random grain boundary free from dispersoids was also grown by the Bridgman method and this will be referred to as sample P.

All the samples I, II and P were spark-cut to obtain tensile specimens with cross-sectional area 1.2 mm × 2.0 mm and gauge length 5.5 mm. The specimens were cut so that the grain boundary was oriented 45° to the tensile axis and located at the middle of the specimen,

* *Present address*: Department of Engineering Science, Faculty of Engineering, Kyoto University, Kyoto 606, Japan.
‡ *Present address*: Department of Mechanical Engineering and Materials Science, Yokohama National University, Tokiwadai, Hodogaya-ku, Yokohama 240, Japan.

0022–2461/88 $03.00 + .12

TABLE I Distribution of SiO_2 particles on grain boundaries for Cu–SiO_2 samples I and II

	Particle radius, r (μm)	Area fraction, A (%)
Sample I	0.16	31
Sample II	0.23	24

as shown in Fig. 1. Before the mechanical test, all the specimens were annealed at 1073 K for 8.64×10^4 sec and electrolytically polished.

2.2. Tensile test

Using an Instron-type testing machine, the specimens were deformed in tension at various temperatures between 450 and 1050 K in an argon atmosphere. In order to minimize the rotation of the crystals caused by the shear deformation on slip planes and grain boundaries, two specimens cut from the same bicrystal were connected in series with a joint, as shown in Fig. 1. The weight of the joint (5.5 g) is negligible compared with the applied load. Because the two specimens aligned in series have the same cross-sectional area, crystal orientation and grain-boundary orientation, and because the specimens exhibit work-hardening, as will be seen later, it can be expected that the two specimens continue to deform in practically the same manner.

A cross-head speed of 1.7×10^{-6} m sec^{-1} was employed as a deformation rate. This corresponds to the initial strain rate of 1.5×10^{-4} sec^{-1}.

2.3. Microstructural observation

The fracture surfaces of specimens were observed on a scanning electron microscope (SEM). In addition, an optical microscope was used to examine the surfaces and the longitudinal sections of the other specimens in series which did not fracture. When fracture occurs at a grain boundary in one of the specimens, such observation enables us to reveal the microstructure of the grain boundary just before fracture in the other pre-fractured specimen.

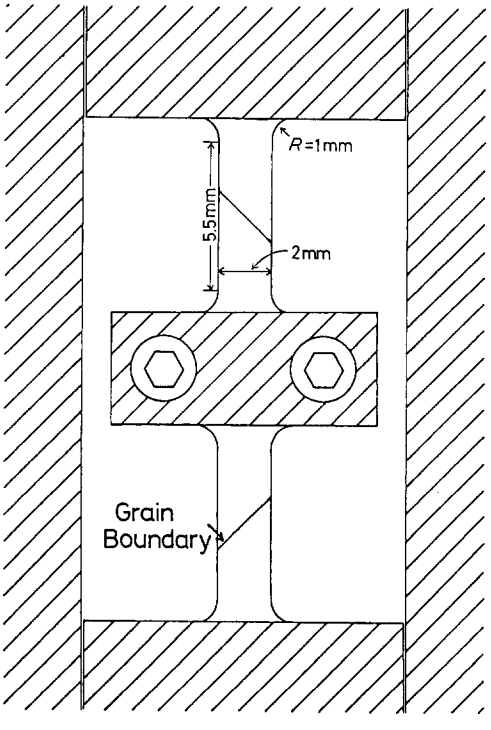

Figure 1 Two bicrystals connected in series were tensile tested as shown in order to minimize the rotation of crystals. Upper and lower bicrystals were cut from the same original sample.

3. Results

3.1. Fracture modes

Figs 2a, b and c show nominal stress–nominal strain curves for specimens I, II and P, respectively, obtained at various temperatures. By comparing Figs 2a, b and c, it can be found that although the total elongation of specimens I and II decreases distinctly with increase in temperature, that of specimen P does not change very much. In the case of specimen P, the fracture mode was transgranular at all tested temperatures. However, in the case of specimens I and II, intergranular fracture was observed except for specimen I deformed at 450 K.

In order to reveal the difference in the fracture mode between pure copper and Cu–SiO_2 alloys, the microstructure near the grain-boundaries of the pre-fractured bicrystal specimens was observed after deformation. Figs 3a and b show optical micrographs of the grain-boundary morphology just before the fracture for specimens I and P deformed at 750 K. In specimen P, extensive recrystallization is observed and the original grain boundary has disappeared (Fig. 3a). However, in specimen I, although grain-boundary sliding is detected by the relative shift in scratches on the surface, recrystallization is not observed and the grain boundary is located as it was (Fig. 3b).

3.2. Intergranular fracture

Specimen II fractured in a more brittle manner than specimen I at any tested temperature (Figs 2b and c). The main difference between the two bicrystals is the crystal orientations of the grains. Figs 4a and b show stereographic projections indicating the tensile directions, the grain-boundary planes and the primary slip directions of grains A and B for specimens I and II.

To examine the origin of the difference in the fracture behaviour between specimens I and II, the fracture surfaces were observed by SEM. Figs 5a and b show the fracture surfaces of specimens I and II deformed at 450 K. At this temperature, the fracture mode of specimen I is transgranular and that of specimen II is intergranular. Both fracture surfaces are made of elongated dimples which are considered to have formed by the growth and coalescence of grain-boundary voids nucleated near the SiO_2 particles [3, 5]. In-grain particles are smaller than grain-boundary particles, as can be compared in Figs 5a and b.

Above 550 K, both specimens I and II show the intergranular fracture. However, the microscopic features of the fracture mode are different. An example of the difference is seen when the specimens were deformed at 550 K. Fig. 6a shows the fracture surface of specimen I deformed at 550 K. The ledges corresponding to the traces of the primary slip planes are the characteristic features of this fracture mode. On the other hand, the fracture surface of specimen II deformed at

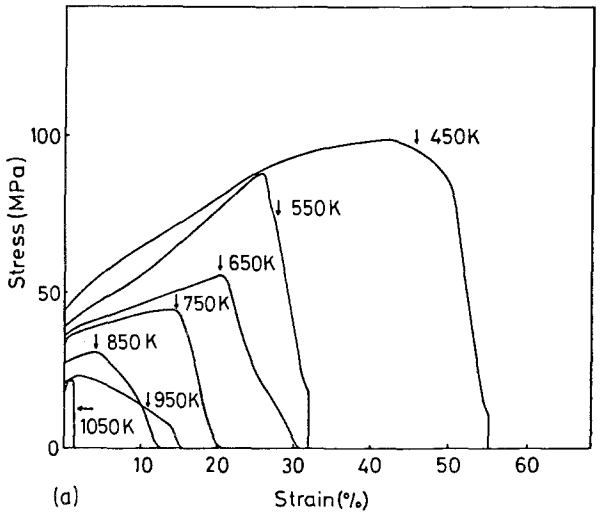

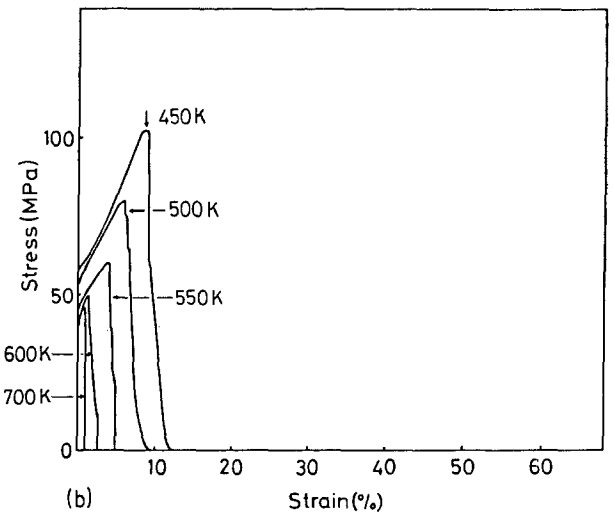

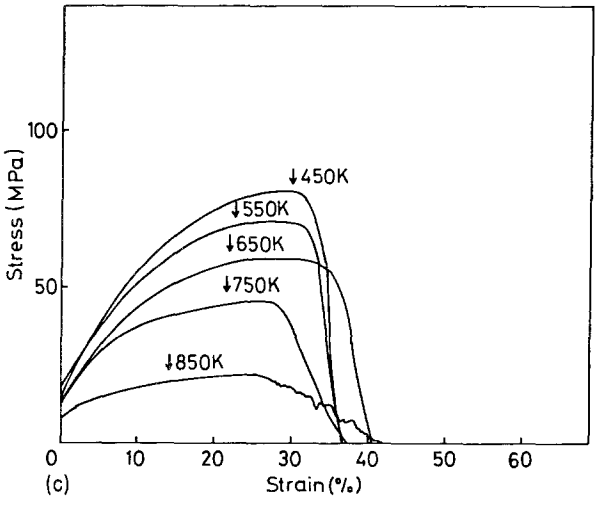

Figure 2 Stress–strain curves of (a) specimen I, (b) specimen II, and (c) specimen P, deformed at various temperatures (strain rate = $1.5 \times 10^{-4}\,\mathrm{sec}^{-1}$).

550 K is made of shallow grain-boundary dimples containing SiO_2 particles, as shown in Fig. 6b. This difference in the fracture mode was commonly observed in specimens I and II in the temperature range 500 to 700 K.

4. Discussion

4.1. Difference in fracture mode and ductility between Cu–SiO_2 alloys and pure copper

Results of microstructural observation and tensile tests indicate the occurrence of intergranular fracture for specimens I and II deformed at and above 550 K. The temperature above which the intergranular fracture and the loss of ductility occur corresponds well to the temperature at which the grain-boundary sliding is first detected from the shift in surface scratches on the deformed specimen surfaces. On the other hand, specimen P maintains fairly good ductility and its fracture mode is invariably transgranular up to 850 K. Hence, it can be concluded that the SiO_2 particles on the sliding grain boundaries play an important role in the high-temperature embrittlement. Of course, in specimen P, the grain-boundary sliding also occurs

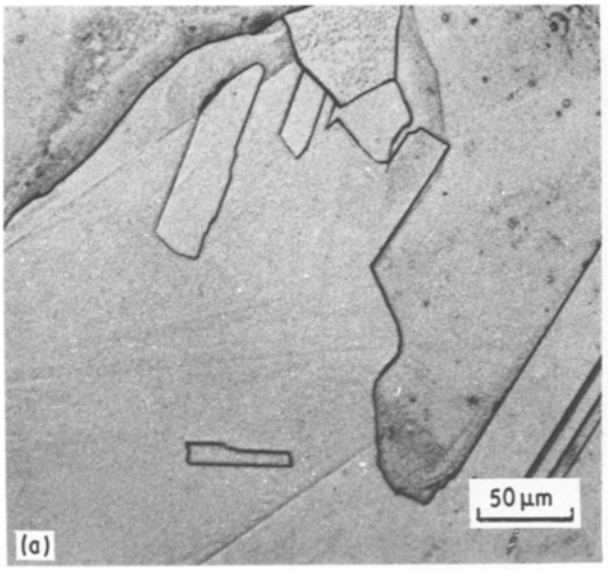

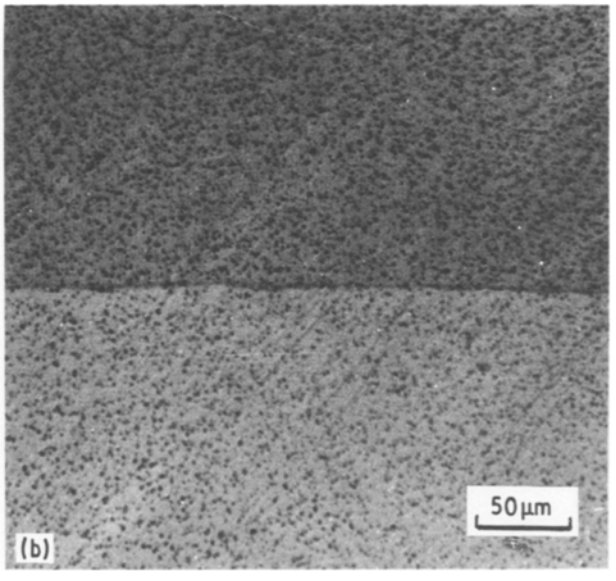

Figure 3 Optical micrographs showing the grain-boundary morphology after deformation. (a) Specimen P and (b) specimen I deformed at 750 K.

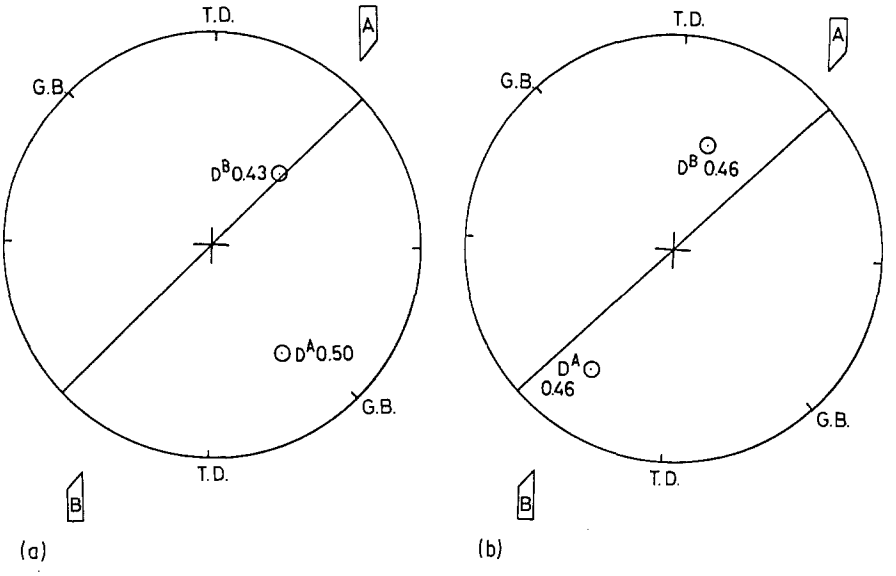

Figure 4 Stereographic projections showing tensile directions (TD), grain-boundary planes and primary slip directions (D^A and D^B) of grains A and B for (a) specimen I, and (b) specimen II. The Schmid factors of primary slip systems are also indicated.

during the initial stage of deformation. Because of the absence of grain-boundary particles, sliding is expected to occur easier in specimen P than in specimens I and II [7, 8]. However, as shown in Fig. 3, recrystallization around the grain boundary takes place extensively in specimen P. The recrystallization causes the rearrangement of atoms in the locally deformed grain boundary and relieves the stress concentration [5, 9]. In contrast, recrystallization is absent in specimens I and II and stress concentration appears at the periphery of SiO_2 particles on the sliding grain boundary. By considering that such stress concentration near the particles provides the preferential sites for the initiation of fracture [2, 3, 5, 10], the difference in the fracture mode between Cu–SiO_2 and pure copper is reasonably explained.

The temperature dependence of ductility for specimens I and II can also be explained in a similar manner. The grain-boundary sliding becomes easier as temperature becomes higher. Therefore, the stress concentration near the SiO_2 particles becomes more significant at higher temperatures, thereby leading to the more brittle fracture [2, 3, 5, 10].

4.2. Recrystallization during deformation

Here, the difference in the recrystallization behaviour between bicrystals of Cu–SiO_2 alloys and pure copper will be discussed. It was found in the present experiment that the SiO_2 particles on grain boundaries severely retard the recrystallization near the grain boundaries. Two seemingly conflicting explanations have been made for the effect of dispersed particles on recrystallization. One is based on the stress concentration near the particles. That is, the stress concentration near the particles is considered to provide a driving force for recrystallization [11]. The other is based on the pinning effect of particles on the grain-boundary migration. That is, the particles are considered to impede recrystallization by reducing the mobility of grain boundaries [12, 13]. Taking into account the Zener relationship for the grain-boundary pinning [12] and the experimental results given by previous investigations [14, 15], Beden [1] has presented a criterion for the size and distribution of dispersed particles to judge whether or not the particles in a matrix retard the recrystallization. According to his results, if $A/r > 3 \times 10^5\,m^{-1}$ is satisfied, the particles on grain

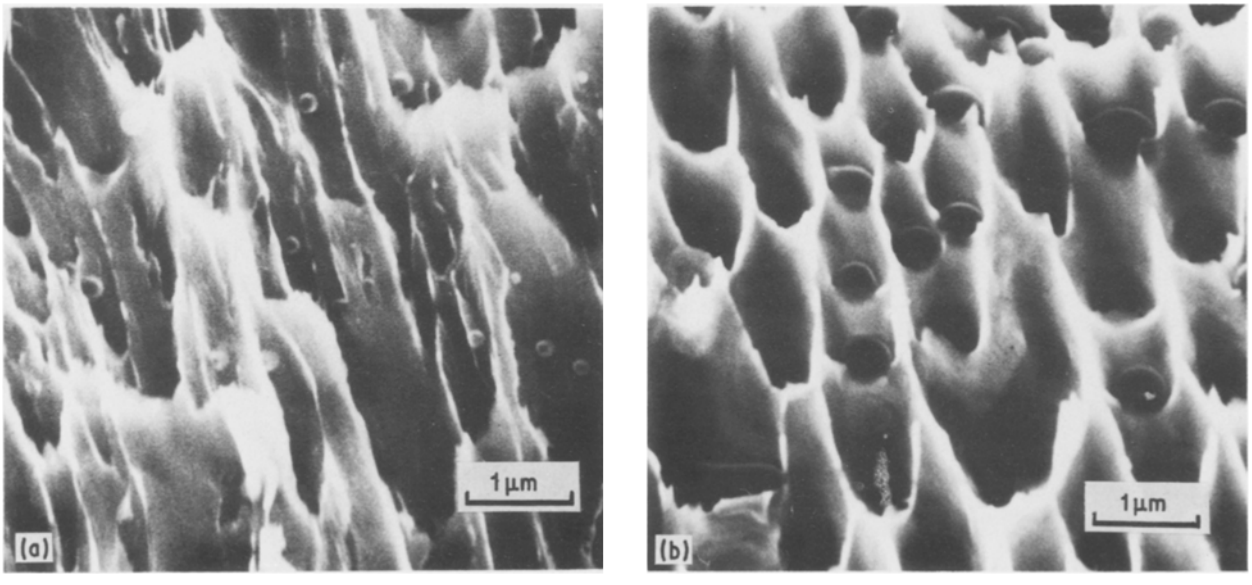

Figure 5 Scanning electron micrographs of fracture surfaces for (a) specimen I, and (b) specimen II, deformed to failure at 450 K.

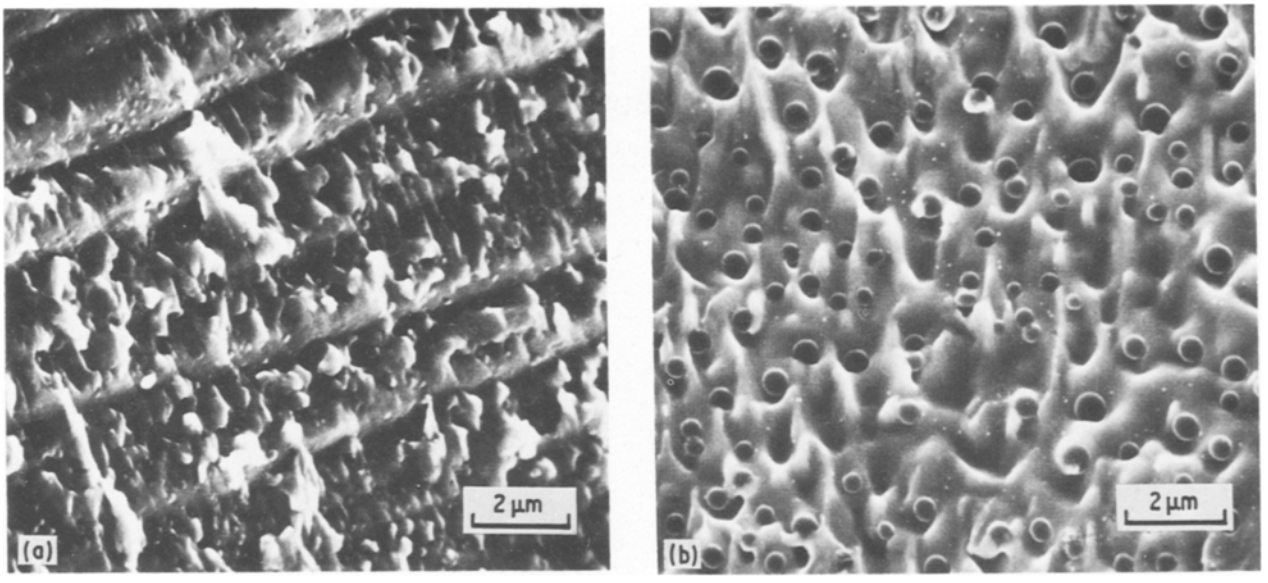

Figure 6 Scanning electron micrographs of fracture surfaces for (a) specimen I, and (b) specimen II, deformed to failure at 550 K.

boundaries retard the recrystallization (A = the area fraction of the particles on grain boundaries, r = the grain-boundary particle radius). Using the values of A and r in Table I, it is found that the calculated values for specimens I and II are $A/r = 1.9 \times 10^6 \text{m}^{-1}$ and $1.0 \times 10^6 \text{m}^{-1}$, respectively. Both values are greater than $3 \times 10^5 \text{m}^{-1}$, and this reasonably supports the results of the present study that recrystallization was not observed in the Cu–SiO_2 bicrystals but was observed in the pure copper bicrystals.

The deformation and fracture behaviour of Cu–GeO_2 polycrystals has been examined through tensile tests by Onaka *et al.* [5]. Contrary to the present results, Cu–GeO_2 polycrystals have exhibited extensive recrystallization during deformation at temperatures around 700 K under a strain rate of 10^{-4}sec^{-1}, and the recovery of ductility has occurred in this temperature range. Because Onaka *et al.* used polycrystals, the applied stress level was higher than that in the present study. This should presumably affect the recrystallization behaviour. More importantly, however, it can be pointed out that the difference in the recrystallization behaviour is reasonably attributed to the difference in the distribution of grain-boundary particles. In the case of Cu–GeO_2 polycrystals which Onaka *et al.* have examined, the values of A/r are $1.5 \times 10^5 \text{m}^{-1}$ and $1.8 \times 10^5 \text{m}^{-1}$. These values are smaller than those of specimens I and II and the critical value, $3 \times 10^5 \text{m}^{-1}$. Therefore, the observed enhancement of recrystallization in the Cu–GeO_2 alloy can be understood.

4.3. Comparison between specimens I and II

Specimens I and II which have almost the same size and distribution of particles have shown quite different behaviour in ductility, as shown in Figs 2a and b. By taking into account that the grain-boundary sliding is closely related to the intergranular fracture, it can be considered that the amount of grain-boundary sliding is different between specimens I and II. As recrystallization can be retarded, dispersion-hardened alloys are in a sense suitable for the examination of the intrinsic nature of grain-boundary sliding at intermediate temperatures.

In the case of special boundaries with low Σ values, grain-boundary sliding is known to be very difficult [16]. However, as both specimens I and II have random boundaries, the difference in the deformation and fracture behaviour cannot be explained through the intrinsic difference in the grain-boundary structure. Therefore, we will consider the possible difference in the relative contribution of in-grain deformation to the total deformation.

The effects of the in-grain deformation on the grain-boundary sliding have been theoretically studied by McLean [17] and his model has been modified by Watanabe and Davies [18]. They have considered that the sliding is the result of the movement of lattice dislocations along the grain boundary. If we restrict ourselves to the primary slip systems by assuming that they are the only operative slip systems during deformation, the following rate equation of grain-boundary sliding can be presented [17, 18].

$$\dot{S} \propto m_A F_A b_{pA} + m_B F_B b_{pB}$$

$$F = f_n \pm f_p$$

$$= \sigma_n b_n \pm \tau b_p$$

where, $\dot{S}$ is the rate of grain-boundary sliding, m the Schmid factor, b_n and b_p the resolved components of the Burgers vector normal and parallel to the grain boundary, respectively, and σ_n and τ the resolved shear and normal components of the applied stress, respectively (see Fig. 7). Subscripts A and B denote the grain A and grain B which constitute a bicrystal.

Using the stereographic projections shown in Figs 4a and b, the ratio of the rates of grain-boundary sliding for specimen II, $\dot{S}_{II}$ and for specimen I, $\dot{S}_I$, can be obtained. The calculation reveals that the ratio $\dot{S}_{II}/\dot{S}_I$ is 1.2. This means that the contribution of the in-grain dislocations to the grain-boundary sliding is greater for specimen II than for specimen I and that the grain boundary of specimen II can slide more easily compared with that of specimen I. The fracture surface

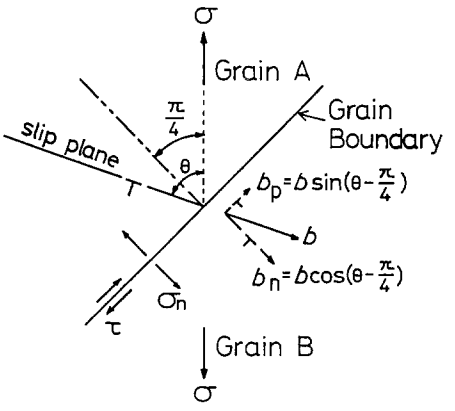

Figure 7 Schematic representation of the dislocation mechanism of grain-boundary sliding and grain-boundary dislocations generated from in-grain dislocations.

observation mentioned earlier also supports this result; the fracture surfaces observed for specimens II are made of elongated grain-boundary voids which are considered to have been nucleated and grown as the grain-boundary sliding occurs (Fig. 6b) [5]. On the other hand, the ledges are observed on the fracture surfaces of specimens I. These ledges must have been formed as a result of pile-up of dislocations at the grain boundaries.

Because the dislocations on the primary slip planes in specimens II can glide and climb along the boundary more easily compared with specimens I, stress concentration near the grain-boundary SiO_2 particles is more easily developed, leading to the more significant brittle fracture in specimens II.

The above discussion may be too simplified as slip lines belonging to other slip systems were also observed. However, we believe that the essential difference in the deformation behaviour between specimens I and II certainly comes from the interaction between the in-grain deformation and the grain-boundary sliding.

Acknowledgements

This research was supported by a Grant-in-Aid for Scientific Research from the Ministry of Education, Science and Culture under Contract 60420046 and also by a Science and Technology Grant from the Toray Science Foundation.

References

1. I. BEDEN, *Scripta Metall.* **20** (1986) 1.
2. H. RIEDEL, *Acta Metall.* **32** (1984) 313.
3. A. S. ARGON, in "Recent Advances in Creep and Fracture of Engineering Materials and Structures", edited by B. Wilshire and D. R. J. Owen (Pineridge, Swansea, 1981) p. 1.
4. W. PAVINICH and R. RAJ, *Metall. Trans.* **8A** (1977) 1917.
5. S. ONAKA, M. KATO and R. TANAKA, *Trans. J. Inst. Metals* **28** (1987) 32.
6. D. G. BRANDON, *Acta Metall.* **14** (1966) 1479.
7. T. MORI, M. KODA, R. MONZEN and T. MURA, *ibid.* **31** (1983) 275.
8. S. ONAKA, M. KATO and T. MORI, *Metall. Trans.* **17A** (1986) 1949.
9. M. F. ASHBY, in "Proceedings of a Conference on Fracture Mechanics", edited by R. A. Smith (Cambridge University Press, 1971), p. 1.
10. R. RAJ and M. F. ASHBY, *Acta Metall.* **23** (1975) 653.
11. M. F. ASHBY, *Philos. Mag.* **21** (1969) 399.
12. C. ZENER, personal communication (1948), to C. Smith, *Trans. AIME* **175** (1948) 15.
13. E. GRANT, A. PORTER and B. RALPH, *J. Mater. Sci.* **19** (1984) 3554.
14. R. D. DOHERTY and J. W. MARTIN, *J. Inst. Metals* **91** (1962–63) 332.
15. O. K. CHOPRA and P. NIESSEN, *J. Mater. Sci.* **9** (1974) 279.
16. H. KOKAWA, T. WATANABE and S. KARASHIMA, *Philos. Mag.* **A44** (1981) 1239.
17. D. McLEAN, *ibid.* **23** (1971) 467.
18. T. WATANABE and P. W. DAVIES, *ibid.* **A37** (1978) 649.

Received 23 March
and accepted 3 June 1986